Published in final edited form as:
Cell Mol Bioeng. 2008 December 1; 1(4): 229–239. doi:10.1007/s12195-008-0028-4.

Surface Plasmon Resonance Monitoring of Cell Monolayer Integrity: Implication of Signaling Pathways Involved in Actin-Driven Morphological Remodeling

Charles M. Cuerrier[1], **Vincent Chabot**[1,2], **Sylvain Vigneux**[1], **Vincent Aimez**[2], **Emanuel Escher**[1], **Fernand Gobeil Jr.**[1], **Paul G. Charette**[2], and **Michel Grandbois**[1]

[1] Département de Pharmacologie, Université de Sherbrooke, 3001 12th Avenue North, Sherbrooke, QC, Canada J1H 5N4

[2] Département de Génie Électrique et Génie Informatique, Université de Sherbrooke, 2500 Blvd Université, Sherbrooke, QC, Canada J1K 2R1

Abstract

Morphological changes occurring in individual cells largely influence the physiological functions of various cell layers. The control of barrier function of epithelia and endothelia is a prime example of processes highly dependent on cellular morphology and cell layer integrity. Here, we applied the surface plasmon resonance (SPR) technique to the quantification of cellular activity of an epithelial cell monolayer stimulated by angiotensin II. The analysis of the SPR signal shows reproducible concentration-dependent biphasic responses after cell activation with angiotensin II. Phase-contrast and confocal microscopy imaging was performed to link the SPR signal to molecular and global morphological remodeling. The SPR signal was observed to be in relation with the rapid cell contraction and the subsequent cell spreading observed by phase-contrast microscopy. Additionally, the temporal redistribution of actin, observed by confocal microscopy after angiotensin II stimulation, was also found to be consistent with the SPR signal variation. The modulation of signaling pathways involved in actin-myosin driven cell contraction confirms the direct implication of actin structures in the SPR response. Additionally, we show that the intracellular calcium mobilization associated with angiotensin II stimulation did not produce any significant SPR signal variation. Altogether, our results demonstrate that SPR is a rapid label-free method to study cellular activity and molecular mechanisms implicated in the modulation of the integrity of a cell monolayer in relation to cytoskeleton remodeling with associated cell morphological changes.

Keywords

Surface plasmon resonance; Cell layer integrity; Angiotensin II; Cell morphology; Cell signaling

INTRODUCTION

The epithelial cell layer cohesion is a key player in the control and maintenance of tissue homeostasis. Although the range of experimental approaches applied to the study of physiological processes involving epithelium permeability is extensive,[1,31,37,43,47] there is still a need for label-free techniques that allow precise time-resolved informations on the cell molecular activity implicated in cell morphology changes. To date, cell and intracellular

Address correspondence to Michel Grandbois, Département de Pharmacologie, Université de Sherbrooke, 3001 12th Avenue North, Sherbrooke, QC, Canada J1H 5N4. michel.grandbois@usherbrooke.ca.

molecular activities are routinely monitored through different techniques such as fluorescence microscopy or molecular assay reporting concentration or activation of various cellular components such as the intracellular calcium concentration, cyclic-AMP, actin cytoskeleton reorganization or the activation of several kinases and phosphatases.[2,4,5,10] These assays rely on molecular labels brought from the outside into the cytosol or incorporated to the cell intrinsic biomolecular machinery using the toolbox of molecular biology.

A new emerging application for surface plasmon resonance (SPR), a technique largely employed in molecular bioassays,[19] is the analysis of cellular processes. With its exquisite precision to determine mass variations occurring in the vicinity of a gold surface, this technique is of interest to analyze phenomena occurring in the first 200 nm above the studied sample. As suggested by Hide *et al.* in 2002, SPR might have the capacity to detect a variety of cellular processes. Indeed, SPR was applied to the study of the ligand-induced reaction of mast cells,[17,45] apoptotic response[45] and the detection of blood coagulation and platelet adhesion.[15] SPR has also allowed the study of molecular systems isolated from cells, such as actin myosin attachment/detachment in intact sarcomeres,[48] protein–membrane interactions[7] and the cell membrane composition.[51] Furthermore, SPR has provided mechanistic details of calcium-induced selective binding of the calcium-calmodulin complex to a target peptide[32] and other metal ions.[33] These results suggest that SPR can be used to study physiological processes involving molecular changes occurring in the basal region of a cell monolayer due to the activation of specific signaling pathways.

In the SPR technique (Fig. 1a), a p-polarized laser beam is reflected on the sample through a coupling prism at an angle superior to total internal reflection angle. The reflection of the laser beam on the gold-dielectric interface and its coupling with the plasmons generates an evanescent field of hundreds of nanometers above the gold substrate that propagates into the sensing medium containing cells. Optimal coupling between the laser and plasmons is function of the incident angle, the wavelength of the light source and the refractive index of the sensing medium. Therefore, a mass variation within the evanescent field will cause a change in refractive index and will lead to a measurable shift in the angle at which maximum coupling occurs.

Here we used HEK-293 cells, stably expressing the angiotensin II (AngII) AT_1 receptor, as a model to study the relation existing between specific intracellular molecular events and global structural changes involved in cell layer cohesion and integrity. AngII is the active hormone of the renin-angiotensin system which is implicated in many physiological processes, such as vascular contraction as well as sodium and water retention.[11] This agonist, through AT_1 receptors, proceeds via signaling pathways involving the parallel activation of G-proteins as well as small GTPases of the Rho family.[11,13,18,30,34] AT_1 receptor stimulation leads to intracellular Ca^{2+} mobilization and to Rho-Kinase (RhoK) activation.[2,11] These two signaling pathways lead to actin-myosin complex activation through phosphorylation of the myosin light chain (MLC), by the myosin light chain kinase (MLCK) or RhoK,[22,34] which are well known for their implication on the actin myosin molecular motor and the cytoskeleton remodeling. These intracellular events influence the resistance of cells to mechanical perturbation as well as the overall cohesion of cell layers.[13,34,38–40,49]

In this study, we applied the SPR technique to study intracellular molecular mechanisms implicated in the modulation of the integrity of a model cell monolayer. Microscopic observations were performed to validate the implication of cellular components, such as morphological and molecular remodeling, in the SPR signal variation. We demonstrate that SPR can precisely monitor mass changes occurring in the basal portion of a cell monolayer

and that the SPR signal directly correlates with cell morphological modifications, such as intercellular gap formation and cell spreading. These effects are modulated by a variety of cellular and molecular events including cytoskeleton remodeling, cell–cell and cell–substrate adhesion and tension. In addition, using a variety of pharmacological agents in combination with the SPR technique, we were able to evaluate the contribution of the different signaling pathways affecting the actomyosin cell contraction and actin cytoskeleton remodeling induced by AngII activation.

MATERIALS AND METHODS

SPR Gold Surface Preparation

Fisher finest premium microscope glass slides were used as base substrates, which have a refractive index similar to BK7. Prior to metal deposition, glass slides were cleaned in piranha solution (sulfuric acid and hydrogen peroxide 3:1) to remove any contaminants; afterwards they were placed under vacuum for metal deposition (BOC Edwards evaporator, model: AUTO 306). A chromium adhesion layer (3 nm) and a gold layer (48 nm) were deposited subsequently without breaking vacuum between evaporation. Prior to cell culture, SPR glass-gold surfaces were coated with poly-L-lysine (Sigma, Oakville, ON) to assure good cell adhesion.

Cell Culture and Transfection

The transfection of human embryonic kidney-293 (HEK-293) cells (Qbiogene Carlsbad, CA, USA, QBI-HEK- 293A cells), expressing the human AT_1 receptor together with a G-418 resistance gene, was established as previously described[3] (gift from Dr. Gaétan Guillemette, Department of Pharmacology, Université de Sherbrooke). The G-418-resistant clonal cell line was maintained in DMEM supplemented with 10% heat-inactivated fetal bovine serum (FBS), 2 mM L-glutamine, 2.5 μg/mL amphotericin B, 50 IU/mL penicillin, 50 μg/mL streptomycin (Wisent, St-Bruno, QC, Canada) and 0.4 mg/mL G-418 (Gibco Life Technologies, Gaithersburg, MD, USA) at 37 °C in 5% CO_2 incubator. Depending on the experiment realized, cells were grown to confluence on 3 different substrates: gold poly-lysine coated glass (SPR experiments), normal plastic Petri (phase-contrast experiments) and Petri with poly-lysine coated glass bottom (confocal experiments). Comparison of phase-contrast micrographs obtained for these three different substrates shows no difference in cell adhesion and the cellular response normally observed upon stimulation of the cells. HEK-293 cells were activated with AngII (100 nM) (American Peptide, Sunnyvale, CA, USA) or carbachol (10 μM) (Sigma).[26] To study the contribution of the different signaling pathways, the cells were treated with the inhibitor of myosin light chain kinase ML-9 (20 μM, 30 min), the selective inhibitor of Rho-associated protein kinase Y-27632 (10 μM, 24 h) or the inhibitor of myosin-II-dependent cellular processes blebbistatin (100 μM, 30 min) (Calbiochem, San Diego, CA, USA) for indicated periods of time. To question the implication of AT_1 receptor activation, the cells were treated with the AT_1 antagonist EXP3174 (4 μM) for 10 min (Sigma–Aldrich, Oakville, ON, Canada).

Transfection of HEK-293 cells with GFP-actin was done using the FuGENE 6 transfection reagent protocol (Roche, USA). Briefly, 2 μL of FuGENE 6 was combined with 98 μL serum-free DMEM medium and then mixed with 1 μg of plasmid GFP-actin DNA (gift from Dr. Jean-Luc Parent, Department of Rheumatology, Université de Sherbrooke). After 20 min of incubation at room temperature, the solution was added to the cell-culture Petri dish and incubated for 48 h in 37 °C in 5% CO_2 incubator.

SPR Analysis

The analysis was performed at room temperature on a custom-built surface plasmon resonance apparatus. The sample (n: 1.517; described above) was placed on top of a BK7 coupling prism (n: 1.515; Melles Griot, USA) with a layer of refractive index matching fluid (n: 1.514; Cargille Laboratories, NJ, USA). The cells were incubated in HEPES-Buffered Salt Solution (HBSS) (20 mM Hepes at pH 7.4, 120 mM NaCl, 5.3 mM KCl, 0.8 mM $MgSO_4$, 1.8 mM $CaCl_2$, and 11.1 mM dextrose) during SPR experimentation. A 4 mW laser diode centered at a wavelength of 635 nm (Thorlabs, Inc., USA) was reflected off the sample and passed through a motorized linear polarizer. The laser angle is manually fixed prior the experiments by laser calibration of the apparatus (71.97 ± 0.07°). The intensity of the polarized laser beam was measured with a voltagebiased photodetector (Thorlabs, Inc., USA) and the signal was acquired and treated in a custom-developed LabVIEW control interface program. As only the p-polarization of the laser light is affected by the surface plasmons, the s-polarization was used as a normalization to remove the dependence on laser power drift and other time-dependent noise sources. Results were plotted in reflectance variation units (RVU) where 1 RVU represents 0.1% variation in total reflectance.

Phase-Contrast Microscopy

The morphological changes of the cell were observed by phase-contrast microscopy in a different set of experiments. Briefly, HEK-293 cells, grown on 60 mm Petri dishes, were washed once and the growth medium replaced with HBSS before cell stimulation. The cell morphology changes were recorded using an inverted fluorescence microscope (AxioVert 200, Carl Zeiss, Germany) equipped with a phase-contrast system. All images were captured with a 40× phase-contrast objective, a high-sensitivity camera (AxioCam MRm, Carl Zeiss, Germany) and analyzed with AxioVision LE software.

Confocal Microscopy

The actin cytoskeleton reorganization of the cells expressing GFP-actin was analyzed from confocal microscopy images. HEK-293 cells, grown on 60 mm glass bottom Petri dishes coated with poly-D-lysine, were washed once and the growth medium replaced with HBSS. The cells were examined with a scanning confocal microscope (FLUOVIEW FV1000, Olympus, PA, USA) using a 40× oil-immersion objective. GFP-actin was excited at a wavelength of 488 nm and its emission recorded at 505 nm. Each cell was analyzed in 55 optical sections of 250 nm at every 15 s for 40 min after the stimulation with AngII (100 nM). The resulting image sequence was analyzed using Image-Pro Plus software (MediaCybernetics, Inc., MD, USA).

Cytosolic Calcium Monitoring

HEK-293 cells were washed twice with HBSS and loaded with HBSS + FURA 2/AM (5 μM, Calbiochem, USA) for 20 min at room temperature in the dark. The cells were then washed once and incubated in HBSS alone for 20 min to ensure complete hydrolysis of the FURA 2/AM. The fluorescence intensity of FURA 2/AM-loaded cells was measured by excitation wavelengths of 340 ± 10 nm and 380 ± 10 nm and recorded at 510 ± 40 nm (Carl Zeiss). Cytosolic calcium release was recorded for 30 min at intervals of 3 s. All images for calcium quantification were captured with an Axiovert inverted microscope (Carl Zeiss, Thornwood, NY) fitted with an Attofluor Digital Imaging and Photometry System (Attofluor Inc., Rockville, MD).

Statistics

Data are shown as mean value ± standard error of the mean (s.e.m.). To determine significance of differences ($p<0.05$), we used an analysis of variance (ANOVA) between the groups and a post-hoc (Dunnett correction) to compare each mean with the control group.[29]

RESULTS

SPR Reflectance Variations of a Cell Monolayer Induced by AngII Stimulation

In this study, we used a custom SPR apparatus to monitor cellular activities in HEK-293 cells transfected with the AngII receptor AT_1. These cells have been previously demonstrated to respond to AngII by optical microscopy[4] and through the monitoring of intracellular calcium mobilization.[2] For all SPR experiments, cells were grown on disposable gold-coated glass slides until confluence, following which the glass slides were mounted onto the BK7 prism of the SPR apparatus (Fig. 1a). Figure 1b presents a typical SPR response induced by AT_1 receptor activation with 100 nM AngII. The SPR signal was plotted as reflectance variation units (RVU) as a function of time (min). The baseline prior to the injection of AngII showed a constant plateau (I in Fig. 1b), which is consistent with a steady-state level of cellular activity. Immediately after the stimulation by AngII, a rapid diminution in the SPR signal was observed and reached a mean minimum value of 28.06 ± 5.53 RVU ($n = 5$), approximately 2 min after stimulation (II in Fig. 1b). The cellular response was subsequently followed by an increase of the SPR signal that gradually exceeded the baseline value (III in Fig. 1b). In Fig. 1c, we present control experiments conducted to confirm that the observed SPR response was the result of the AT_1 receptor activation by AngII. At first, we only stimulated the cells with the vehicle (HBSS) to address the possibility of an SPR response induced by the addition of liquid in the fluid chamber or an indirect cellular stimulation by shear stress. As expected, no SPR signal variation was observed after the injection of HBSS (Fig. 1c). In addition, to directly question the implication of the AT_1 receptor activation in the SPR signal response, we pretreated the cells with the AT_1 antagonist EXP3174. A complete abolition of the AngII-induced response was observed in presence of the antagonist, thus confirming the implication of the AT_1 receptor in the recorded signal (Fig. 1c).

Figure 2a shows the SPR signal associated with the stimulation of cells by different AngII concentrations (1, 10 and 100 nM). We can see that an increase in the AngII concentration affects the magnitude of initial SPR response following cell activation. Hence, the magnitude of the initial response (Fig. 2b, inset) was used to generate a dose–response histogram of the AngII receptor activation. As expected, increasing the concentration of AngII, from 1 pM to 10 μM, caused a concentration-dependent RV, reaching a maximum response at 100 nM AngII (Fig. 2b).

Effects of Cell Morphology Modifications on SPR Reflectance Variations

SPR is by definition sensitive to mass changes occurring in the vicinity of the gold-sensing surface. For this reason it is expected to be particularly sensitive to any cell morphological change. To test this possibility, cell morphology variations in time were observed by phase-contrast microscopy and compared with the SPR signal (Fig. 3). A careful look at the phase-contrast micrograph of the HEK-293 cell layer, taken before AngII stimulation, revealed a normal morphology with the presence of intercellular space between cells. However, 2 min after the cell stimulation with AngII, a contraction of the cell body was clearly visible with an increase in the intercellular spaces (see Fig. 3a, 2 min). This initial cell response was followed by a spreading of the cells and a consequent decrease of the intercellular spaces. The time course of these morphological changes was found to be very consistent with the

biphasic SPR response. In Fig. 3b, we present a control experiment showing morphologically stable cells before and after stimulation by HBSS without AngII.

Effects of the Cell Actin Cytoskeleton Distribution on SPR Reflectance Variations

As observed by Auger-Messier *et al.* in 2005, AngII stimulation of HEK-293 cells, expressing the AT_1 receptor, induces a major reorganization of the actin cytoskeleton in the apical and basal portions of the cells,[4] which we assume can contribute to the SPR signal variation. HEK-293 cells were co-transfected with GFP-actin and observed with confocal microscopy to evaluate the possible contribution of this actin redistribution on the SPR signal. As shown in Fig. 4a (−2 min), the transversal reconstruction from confocal micrographs of an unstimulated cell shows a somehow uniform distribution of actin structures. In this micrograph, the observed fluorescence signal is generated by both the monomeric and filamentous actin components of the overall actin population. As a result, the background fluorescence signal can be attributed to the monomeric GFP-actin subpopulation. An important feature of the confocal micrograph sequence was the actin redistribution to the apical region of the cell observed 2 min after AngII stimulation. This actin mobilization at the apical region was then gradually followed by a redistribution of actin to the basal region of the cell. In Fig. 4a (2 min), we observed a slight increase in GFP-actin fluorescence in the bottom section of the cell, corresponding to a reorganization of actin structures toward the center of the cell. However, we consider that this increase in actin should not contribute to the SPR signal since the detection is limited to the first 200 nm of the cell. This biphasic fluorescence observation correlates well with the SPR signal variation (Fig. 4b) and suggests that this biphasic redistribution of actin also contributes to the variation in the SPR signal.

Numerous signaling pathways are implicated in actin remodeling and actomyosin-dependent contractions. To validate the implication of actin in cell morphology changes, and thus in the SPR signal generation, we treated the cells with different pharmacological agents targeting specific elements of key signaling pathways. The inhibition of the myosin light chain kinase (MLCK) with ML-9 did not influence the normal SPR signal nor the change in morphology normally observed after cell stimulation with 100 nM AngII. In contrast, RhoK inhibition with Y-27632 repressed both the SPR signal and cell morphological contraction and spreading (Fig. 5b). To further analyze the implication of actin in the SPR signal, we directly interfered with actomyosin contraction by the pretreatment of cells with blebbistatin. Here again, SPR signal changes were completely inhibited, confirming a close relation between actin reorganization and signal variations (Fig. 5c). Figure 5d shows a RV comparison between all pharmacological agents employed in this study, compiled again by measuring the mean initial decrease in the SPR signal.

Effects of the Intracellular Calcium Mobilization on SPR Reflectance Variations

Another important cellular element that could cause a mass variation within the evanescent field and subsequently influence the SPR signal is the intracellular calcium mobilization induced by AngII stimulation.[2] To establish the temporal relationship between the intracellular calcium and the SPR signal, we used the ratiometric fluorescent calcium indicator FURA 2/AM. In Fig. 6a, we present a cytosolic calcium monitoring, which shows a characteristic transitory increase that reaches a maximum a few seconds after AT_1 receptor activation by 100 nM AngII. This calcium release normally returns near the basal level within 5 min after AngII stimulation. The intracellular calcium comparison with the SPR signal shows a certain correlation that could suggest the implication of calcium in the RV. To validate this hypothesis, we stimulated the cell with carbachol (CCh), an agonist known to activate G-protein-coupled muscarinic receptors. [20,26] This agonist induced a calcium increase in the cell, by the same signaling pathway as AngII, but without inducing a cellular

contraction that would be detected here in phase-contrast micrographs (Figs. 6c and 6e). Interestingly, 10 μM CCh did not modify the SPR signal, despite the fact that it induced an intracellular calcium augmentation similar to 100 nM AngII (Fig. 6d).

DISCUSSION

In this study, we demonstrated that molecular activity of a human epithelial cell monolayer, associated with morphological changes, could be followed in real-time using surface plasmon resonance. The origin of the SPR reflectance variations occurring as a result of the cell stimulation with AngII was ascertained using pharmacological agents as well as microscopy techniques. AngII stimulation is well-known to induce the activation of many cellular processes, such as actin cytoskeleton reorganization and intracellular calcium mobilization.[2,4] Both processes play a role in cell contraction and are expected to be closely implicated in the observed SPR signal variations. SPR sensing, following cell stimulation, was previously applied to the monitoring of mast cells stimulated by antigens and was proposed to reflect the assembly of molecules near the plasma membrane.[17] Our analysis takes into account three distinct cell parameters on the SPR signal induced by cell activation by AngII: (1) changes in cellular morphology; (2) actin cytoskeleton reorganization and (3) transitory intracellular calcium mobilization.

The SPR reflectance variation (RV) of a HEK-293 cell monolayer follows a reproducible time course after AngII stimulation, which can be seen as an overall signature of the process. Epithelial and endothelial cells are sensitive to several external stimuli such as an increase in shear stress,[8,16,25] which could potentially induce a cellular response detectable by SPR. As shown in the control, the absence of RV after the addition of the vehicle (HBSS) alone indicates that the shear stress is not responsible for the observed variation in the SPR signal. Furthermore, when the cells are pretreated with the AT_1 receptor antagonist EXP3174, the disappearance of the characteristic AngII-induced SPR response confirms that the signal occurs as a result of receptor activation. In contrast, after AT_1 receptor stimulation we observed a marked concentration-dependent decrease in reflectance immediately after the stimulation, which reaches a minimum after around 2 min. This initial decrease is followed by a gradual increase in reflectance extending to a level significantly higher than the baseline. The stimulation of the AT_1 receptor was previously documented to induce a biphasic morphological modification of HEK-293 cells that is characterized by a cell contraction followed by a spreading of the cell body.[4] As demonstrated in Fig. 3a, we observed a close relationship between the evolution of the SPR signal and the morphological changes observed by phase-contrast microscopy following AngII stimulation. As stated before, the SPR technique is particularly sensitive for the determination of mass changes occurring in the vicinity of a gold-coated surface.[42] Assuming that cellular density is larger than the density of the medium,[24] a decrease in the area occupied by the cells should reduce the overall molecular density in the vicinity of the sensing surface and, as a result, a decrease in the SPR signal should be observed. Comparison of phase-contrast micrographs taken before and after AngII stimulation reveals a decrease in the area of the cells in contact with the surface, thereby causing an increase in the size of the intercellular spaces. After this first contraction phase, we observed a spreading of the cells on the sensing surface until a near complete disappearance of the intercellular spaces. Again here, this morphological change correlates very well with the augmentation of the SPR signal.

Changes in cell morphology occurred due to significant intracellular reorganizations, especially at the level of the cytoskeleton. It has been reported that AngII stimulation induces an extensive reorganization of actin structures leading in cell contraction and spreading.[4] Our confocal microscopy observations of GFP-actin distribution in cells showed that actin is rapidly redistributed in the apical portion of the cell after AngII stimulation. We

propose that this actin displacement, to a higher part of the cell and away from the sensing SPR surface (>200 nm), could be implicated in the SPR response. Additionally, the subsequent redistribution of actin in the basal portion of the cell, which is associated to cell spreading, could also increase the mass in this region and explain the characteristic SPR signal profile. Hence, these results suggest that actin distribution is closely implicated in the SPR signal variation.

To validate the implication of actin in cell morphology changes, and thus in the SPR signal generation, we treated the cells with different pharmacological agents targeting specific elements of key signaling pathways involved in actin remodeling and actomyosin-dependent contractions. First, we targeted the kinase MLCK, which phosphorylates the myosin light chain (MLC) via intracellular calcium augmentation. [46,50] This particular pathway has been recognized as the major actor in muscle cell contraction.[35] In our epithelial cell line, the direct inhibition of MLCK by ML-9 did not influence AngII cell contraction and allowed normal cell spreading as shown by our phase-contrast microscopy images (Fig. 5a). This result has been demonstrated previously by other studies and suggests that this pathway is not the main actor in epithelial cell contraction and spreading.[13,27,36] The second important pathway is the activation of RhoK, which is directly implicated in the MLC phosphorylation [44,50] as well as extensive actin remodeling.[41] The pretreatment of the cells with Y-27632, a RhoK inhibitor, is well known to prevent cell contraction and spreading.[4,14,44] The notable inhibition of the AngII-induced SPR signal suggests that this is the main pathway implicated in the modulation of the SPR response (Fig. 5b). To directly evaluate the contribution of actomyosin contraction in the SPR signal, we pretreated the cells with blebbistatin, an agent known to inhibit myosin-II ATPase activity and lower actinmyosin affinity.[23] Furthermore, this agent has been recognized to rapidly reduce and inhibit actin stress fiber formation.[6,21] The pretreated cells should therefore be incompetent for actomyosin contraction and cytoskeleton reorganization. As expected, Fig. 5c shows a complete inhibition of the AngII-induced response which further validates that actin is implicated in the SPR signal (Fig. 5c).

Variations in ionic concentrations have been demonstrated to influence the SPR signal in a wide variety of experiments.[9,28] In a living cell system, the intracellular ion concentration in the vicinity of the sensing surface could also potentially contribute to the SPR signal by causing a mass variation within the evanescent field. The activation of the AT_1 receptor induces a release of calcium from intracellular pools and an intake from the extracellular medium.[2] In this case, intracellular calcium concentration increases from 50 to 250 nM in a few seconds, as quantified by the cytosolic calcium monitoring. To evaluate if this release could potentially influence the SPR signal observed in our experiments, the cells were stimulated with the agonist carbachol (CCh), which induces a calcium release similar to AngII in HEK-293 cells without any detectable cell contraction (Figs. 6c and 6e). As expected, no variation in the SPR signal was detected in this experiment suggesting that the intracellular calcium concentration increase does not significantly contribute to the characteristic SPR signal observed (Fig. 6d) following AngII stimulation. This affirmation is further supported by the complete inhibition of the AngII-induced SPR response observed with blebbistatin (Fig. 5c), which also involves intracellular calcium mobilization.[12] Therefore, our results clearly demonstrate that, while intracellular calcium mobilization occurs after AngII stimulation, it is not responsible for the observed SPR signal in our cellular model.

In conclusion, we present SPR as a relevant technique that easily allows the study of cell monolayer activities that are preponderantly related to intracellular molecular remodeling leading to detectable morphological changes. It permits the rapid and label-free probing of cytoskeleton reorganization mechanism and cell signaling pathways implicated in the control of cell morphology and cell monolayer integrity. We envision that this novel SPR

application, by its simplicity and precision, will provide a valuable label-free alternative to monitor cellular processes occurring as a result of the modulation of a large variety of signaling pathways. Additionally, this approach will allow the quantitative monitoring of important physiological processes involving the modulation of cell layer integrity such as vascular permeability.

Acknowledgments

The authors would like to thank Nathalie Nguyen for help with calcium measurements. This work was supported by funds from Canadian Institutes of Health Research (E.E., F.G.), Fonds de la Recherche en Santé du Québec (E.E.), Natural Sciences and Engineering Research Council of Canada (V.A., P.C., M.G.) and Fonds Québécois de la Recherche sur la Nature et les Technologies (V.A., E.E., P.C., M.G.).

References

1. Adamson RH, Curry FE, Adamson G, Liu B, Jiang Y, Aktories K, Barth H, Daigeler A, Golenhofen N, Ness W, Drenckhahn D. Rho and rho kinase modulation of barrier properties: cultured endothelial cells and intact microvessels of rats and mice. J Physiol. 2002; 539:295–308. [PubMed: 11850521]
2. Auger-Messier M, Arguin G, Chaloux B, Leduc R, Escher E, Guillemette G. Down-regulation of inositol 1,4,5-trisphosphate receptor in cells stably expressing the constitutively active angiotensin II N111G-AT(1) receptor. Mol Endocrinol. 2004; 18:2967–2980. [PubMed: 15331757]
3. Auger-Messier M, Clement M, Lanctot PM, Leclerc PC, Leduc R, Escher E, Guillemette G. The constitutively active N111G-AT1 receptor for angiotensin II maintains a high affinity conformation despite being uncoupled from its cognate G protein Gq/11alpha. Endocrinology. 2003; 144:5277–5284. [PubMed: 12960024]
4. Auger-Messier M, Turgeon ES, Leduc R, Escher E, Guillemette G. The constitutively active N111G-AT1 receptor for angiotensin II modifies the morphology and cytoskeletal organization of HEK-293 cells. Exp Cell Res. 2005; 308:188–195. [PubMed: 15896777]
5. Bedecs K, Elbaz N, Sutren M, Masson M, Susini C, Strosberg AD, Nahmias C. Angiotensin II type 2 receptors mediate inhibition of mitogen-activated protein kinase cascade and functional activation of SHP-1 tyrosine phosphatase. Biochem J. 1997; 325(Pt 2):449–454. [PubMed: 9230127]
6. Beningo KA, Hamao K, Dembo M, Wang YL, Hosoya H. Traction forces of fibroblasts are regulated by the Rho-dependent kinase but not by the myosin light chain kinase. Arch Biochem Biophys. 2006; 456:224–231. [PubMed: 17094935]
7. Besenicar M, Macek P, Lakey JH, Anderluh G. Surface plasmon resonance in protein-membrane interactions. Chem Phys Lipids. 2006; 141:169–178. [PubMed: 16584720]
8. Carattino MD, Sheng S, Kleyman TR. Epithelial Na+ channels are activated by laminar shear stress. J Biol Chem. 2004; 279:4120–4126. [PubMed: 14625286]
9. Chah S, Yi J, Zare RN. Surface plasmon resonance analysis of aqueous mercuric ions. Sens Actuators B. 2004; 99:216–222.
10. Coraux C, Kileztky C, Polette M, Hinnrasky J, Zahm JM, Devillier P, De Bentzmann S, Puchelle E. Airway epithelial integrity is protected by a long-acting beta2-adrenergic receptor agonist. Am J Respir Cell Mol Biol. 2004; 30:605–612. [PubMed: 14527924]
11. de Gasparo M, Catt KJ, Inagami T, Wright JW, Unger T. International union of pharmacology. XXIII. The angiotensin II receptors. Pharmacol Rev. 2000; 52:415–472. [PubMed: 10977869]
12. Dou Y, Arlock P, Arner A. Blebbistatin specifically inhibits actin-myosin interaction in mouse cardiac muscle. Am J Physiol Cell Physiol. 2007; 293:C1148–C1153. [PubMed: 17615158]
13. Emmert DA, Fee JA, Goeckeler ZM, Grojean JM, Wakatsuki T, Elson EL, Herring BP, Gallagher PJ, Wysolmerski RB. Rho-kinase-mediated Ca2+-independent contraction in rat embryo fibroblasts. Am J Physiol Cell Physiol. 2004; 286:C8–C21. [PubMed: 12967916]
14. Essler M, Retzer M, Bauer M, Heemskerk JW, Aepfelbacher M, Siess W. Mildly oxidized low density lipoprotein induces contraction of human endothelial cells through activation of Rho/Rho kinase and inhibition of myosin light chain phosphatase. J Biol Chem. 1999; 274:30361–30364. [PubMed: 10521411]

15. Hansson KM, Johansen K, Wettero J, Klenkar G, Benesch J, Lundstrom I, Lindahl TL, Tengvall P. Surface plasmon resonance detection of blood coagulation and platelet adhesion under venous and arterial shear conditions. Biosens Bioelectron. 2007; 23:261–268. [PubMed: 17548188]
16. Helmke BP. Molecular control of cytoskeletal mechanics by hemodynamic forces. Physiology (Bethesda). 2005; 20:43–53. [PubMed: 15653839]
17. Hide M, Tsutsui T, Sato H, Nishimura T, Morimoto K, Yamamoto S, Yoshizato K. Real-time analysis of ligand-induced cell surface and intracellular reactions of living mast cells using a surface plasmon resonance-based biosensor. Anal Biochem. 2002; 302:28–37. [PubMed: 11846373]
18. Higuchi S, Ohtsu H, Suzuki H, Shirai H, Frank GD, Eguchi S. Angiotensin II signal transduction through the AT1 receptor novel insights into mechanisms and pathophysiology. Clin Sci (Lond). 2007; 112:417–428. [PubMed: 17346243]
19. Homola J. Present and future of surface plasmon resonance biosensors. Anal Bioanal Chem. 2003; 377:528–539. [PubMed: 12879189]
20. Ishii M, Kurachi Y. Muscarinic acetylcholine receptors. Curr Pharm Des. 2006; 12:3573–3581. [PubMed: 17073660]
21. Ivanov AI I, McCall C, Parkos CA, Nusrat A. Role for actin filament turnover and a myosin II motor in cytoskeleton-driven disassembly of the epithelial apical junctional complex. Mol Biol Cell. 2004; 15:2639–2651. [PubMed: 15047870]
22. Kamm KE, Stull JT. Dedicated myosin light chain kinases with diverse cellular functions. J Biol Chem. 2001; 276:4527–4530. [PubMed: 11096123]
23. Kovacs M, Toth J, Hetenyi C, Malnasi-Csizmadia A, Sellers JR. Mechanism of blebbistatin inhibition of myosin II. J Biol Chem. 2004; 279:35557–35563. [PubMed: 15205456]
24. Liang XJ, Liu AQ, Lim CS, Ayi TC, Yap PH. Determining refractive index of single living cell using an integrated microchip. Sens Actuators A. 2007; 133:349–354.
25. Lopardo ML, Diaz-Sylvester P, Amorena C. The effect of shear stress on the basolateral membrane potential of proximal convoluted tubule of the rat kidney. Pflugers Arch. 2007; 454:289–295. [PubMed: 17219192]
26. Luo D, Broad LM, Bird GS, Putney JW Jr. Signaling pathways underlying muscarinic receptor-induced [Ca2+]i oscillations in HEK293 cells. J Biol Chem. 2001; 276:5613–5621. [PubMed: 11096083]
27. Melton AC, Datta A, Yee HF Jr. [Ca2+] i-independent contractile force generation by rat hepatic stellate cells in response to endothelin-1. Am J Physiol Gastrointest Liver Physiol. 2006; 290:G7–G13. [PubMed: 16123199]
28. Moon J, Kang T, Oh S, Hong S, Yi J. In situ sensing of metal ion adsorption to a thiolated surface using surface plasmon resonance spectroscopy. J Colloid Interface Sci. 2006; 298:543–549. [PubMed: 16458912]
29. Motulsky, HJ. Analyzing Data with GraphPad Prism. San Diego, CA: GraphPad Software Inc; 1999.
30. Neves SR, Ram PT, Iyengar R. G protein pathways. Science. 2002; 296:1636–1639. [PubMed: 12040175]
31. Nobe K, Sone T, Paul RJ, Honda K. Thrombin-induced force development in vascular endothelial cells: contribution to alteration of permeability mediated by calcium-dependent and -independent pathways. J Pharmacol Sci. 2005; 99:252–263. [PubMed: 16272788]
32. Ozawa T, Kakuta M, Sugawara M, Umezawa Y, Ikura M. An optical method for evaluating ion selectivity for calcium signaling pathways in the cell. Anal Chem. 1997; 69:3081–3085. [PubMed: 9253254]
33. Ozawa T, Sasaki K, Umezawa Y. Metal ion selectivity for formation of the calmodulin-metal-target peptide ternary complex studied by surface plasmon resonance spectroscopy. Biochim Biophys Acta. 1999; 1434:211–220. [PubMed: 10525142]
34. Park JK, Lee SO, Kim YG, Kim SH, Koh GY, Cho KW. Role of rho-kinase activity in angiotensin II-induced contraction of rabbit clitoral cavernosum smooth muscle. Int J Impot Res. 2002; 14:472–477. [PubMed: 12494280]

35. Pfitzer G. Invited review: regulation of myosin phosphorylation in smooth muscle. J Appl Physiol. 2001; 91:497–503. [PubMed: 11408468]
36. Renieri G, Choritz L, Rosenthal R, Meissner S, Pfeiffer N, Thieme H. Effects of endothelin-1 on calcium- independent contraction of bovine trabecular meshwork. Graefes Arch Clin Exp Ophthalmol. 2008; 246(8):1107–1115. [PubMed: 18401592]
37. Riethmuller C, Jungmann P, Wegener J, Oberleithner H. Bradykinin shifts endothelial fluid passage from para- to transcellular routes. Pflugers Arch. 2006; 453:157–165. [PubMed: 17047985]
38. Sahai E, Olson MF, Marshall CJ. Cross-talk between Ras and Rho signalling pathways in transformation favours proliferation and increased motility. EMBO J. 2001; 20:755–766. [PubMed: 11179220]
39. Samarin SN, Ivanov AI, Flatau G, Parkos CA, Nusrat A. Rho/Rho-associated kinase-II signaling mediates disassembly of epithelial apical junctions. Mol Biol Cell. 2007; 18:3429–3439. [PubMed: 17596509]
40. Schafer A, Radmacher M. Influence of myosin II activity on stiffness of fibroblast cells. Acta Biomater. 2005; 1:273–280. [PubMed: 16701806]
41. Schmitz AA, Govek EE, Bottner B, Van Aelst L. Rho GTPases: signaling, migration, and invasion. Exp Cell Res. 2000; 261:1–12. [PubMed: 11082269]
42. Schuck P. Use of surface plasmon resonance to probe the equilibrium and dynamic aspects of interactions between biological macromolecules. Annu Rev Biophys Biomol Struct. 1997; 26:541–566. [PubMed: 9241429]
43. Shigematsu S, Ishida S, Gute DC, Korthuis RJ. Bradykinin-induced proinflammatory signaling mechanisms. Am J Physiol Heart Circ Physiol. 2002; 283:H2676–H2686. [PubMed: 12388246]
44. Somlyo AP, Somlyo AV. Signal transduction by G-proteins, rho-kinase and protein phosphatase to smooth muscle and non-muscle myosin II. J Physiol. 2000; 522(Pt 2):177–185. [PubMed: 10639096]
45. Tanaka M, Hiragun T, Tsutsui T, Yanase Y, Suzuki H, Hide M. Surface plasmon resonance biosensor detects the downstream events of active PKCbeta in antigen-stimulated mast cells. Biosens Bioelectron. 2008; 23:1652–1658. [PubMed: 18339533]
46. Tiruppathi C, Ahmmed GU, Vogel SM, Malik AB. Ca2+ signaling, TRP channels, and endothelial permeability. Microcirculation. 2006; 13:693–708. [PubMed: 17085428]
47. Tiruppathi C, Malik AB, Del Vecchio PJ, Keese CR, Giaever I. Electrical method for detection of endothelial cell shape change in real time: assessment of endothelial barrier function. Proc Natl Acad Sci USA. 1992; 89:7919–7923. [PubMed: 1518814]
48. Tong CW, Kolomenskii A, Lioubimov VA, Schuessler HA, Trache A, Granger HJ, Muthuchamy M. Measurements of the cross-bridge attachment/detachment process within intact sarcomeres by surface plasmon resonance. Biochemistry. 2001; 40:13915–13924. [PubMed: 11705381]
49. Totsukawa G, Wu Y, Sasaki Y, Hartshorne DJ, Yamakita Y, Yamashiro S, Matsumura F. Distinct roles of MLCK and ROCK in the regulation of membrane protrusions and focal adhesion dynamics during cell migration of fibroblasts. J Cell Biol. 2004; 164:427–439. [PubMed: 14757754]
50. van Hinsbergh V, van Nieuw Amerongen G. Intracellular signalling involved in modulating human endothelial barrier function. J Anat. 2002; 200:525. [PubMed: 17103720]
51. Ziblat R, Lirtsman V, Davidov D, Aroeti B. Infrared surface plasmon resonance: a novel tool for real time sensing of variations in living cells. Biophys J. 2006; 90:2592–2599. [PubMed: 16399831]

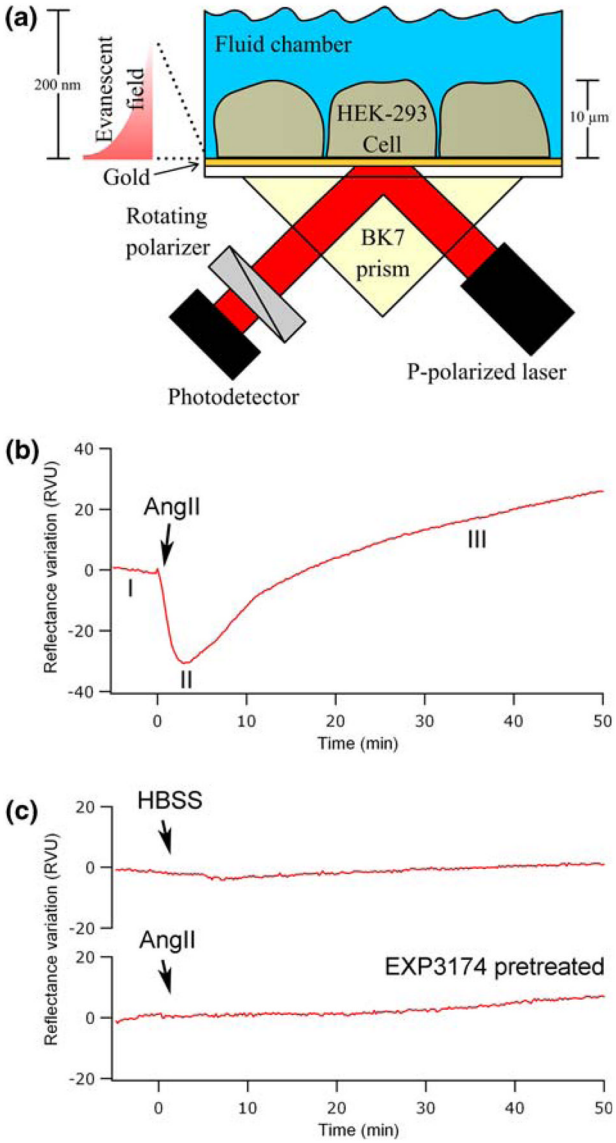

FIGURE 1.

SPR reflectance variations of a cell monolayer induced by AngII activation. (a) Cells were grown on a gold-coated glass slide and placed on top of a BK7 coupling prism with a layer of refractive index matching fluid. A P-polarized laser diode is reflected on the sample and passed through a motorized linear polarizer and the intensity of the polarized laser beam is measured with a voltage-biased photodetector. (b) The SPR signal is plotted as the laser reflectance variation (RV) as a function of time (min). The baseline prior to the injection of 100 nM AngII shows a constant plateau (I), immediately followed by a rapid diminution in the RV signal after the stimulation by AngII (II). The SPR signal then increases to a level exceeding the baseline (III). (c) Control experiments showing SPR response for cells are stimulated with the vehicle (HBSS) or pretreated with an AT_1 antagonist (EXP3174) and stimulated with 100 nM AngII.

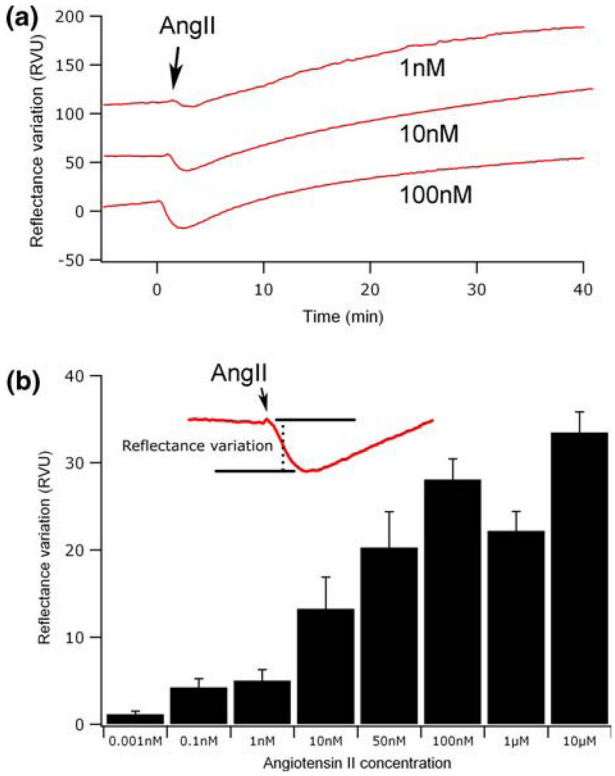

FIGURE 2.

(a) SPR signal measured for increasing AngII concentrations (1, 10 and 100 nM). (b) The amplitude of the initial decrease (inset) was used to generate a concentration response graphic of the AngII receptor activation.

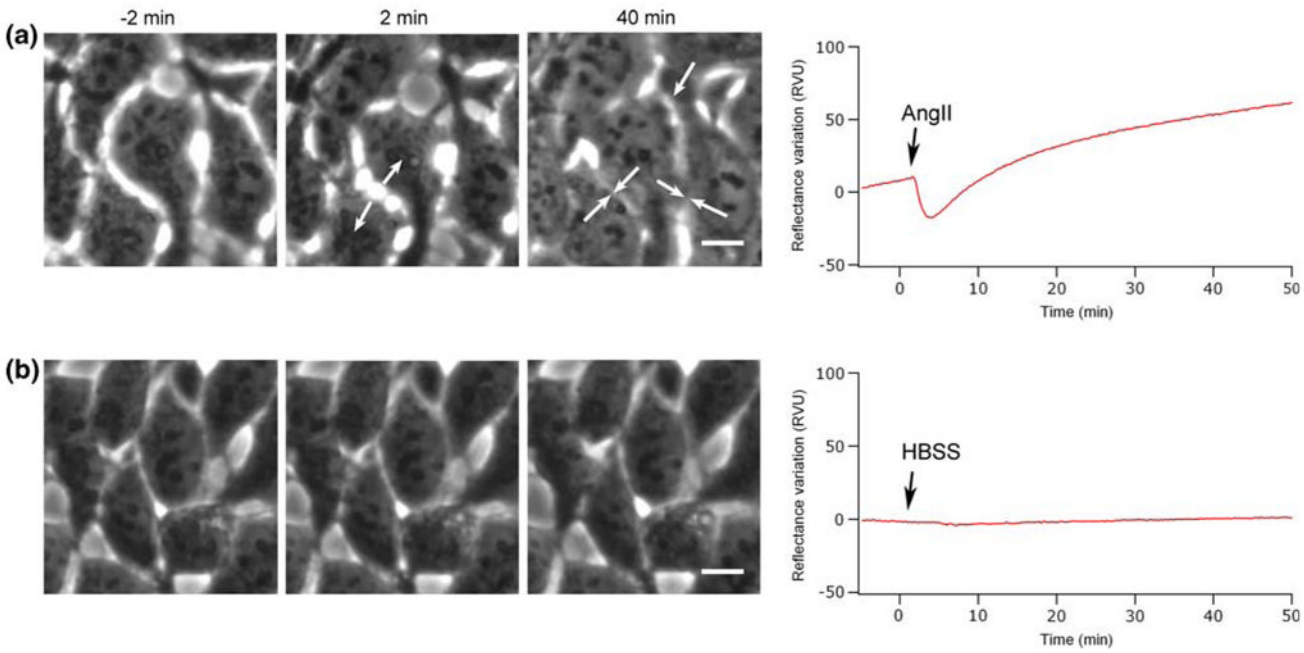

FIGURE 3.

Contribution of cell morphology in SPR reflectance variations. Phase-contrast micrographs recorded before (−2 min) and after cell stimulation (2 and 40 min) with AngII (a) or HBSS (b) are compared with their respective SPR signal variations. The micrograph at 2 min in (a) exhibits a maximum contraction of the cell body (arrows) and corresponds to the maximum in SPR signal decrease. At 40 min, the micrograph shows extensive spreading of the cell, which correlates with the increase of the SPR signal. The scale bars correspond to 10 μm.

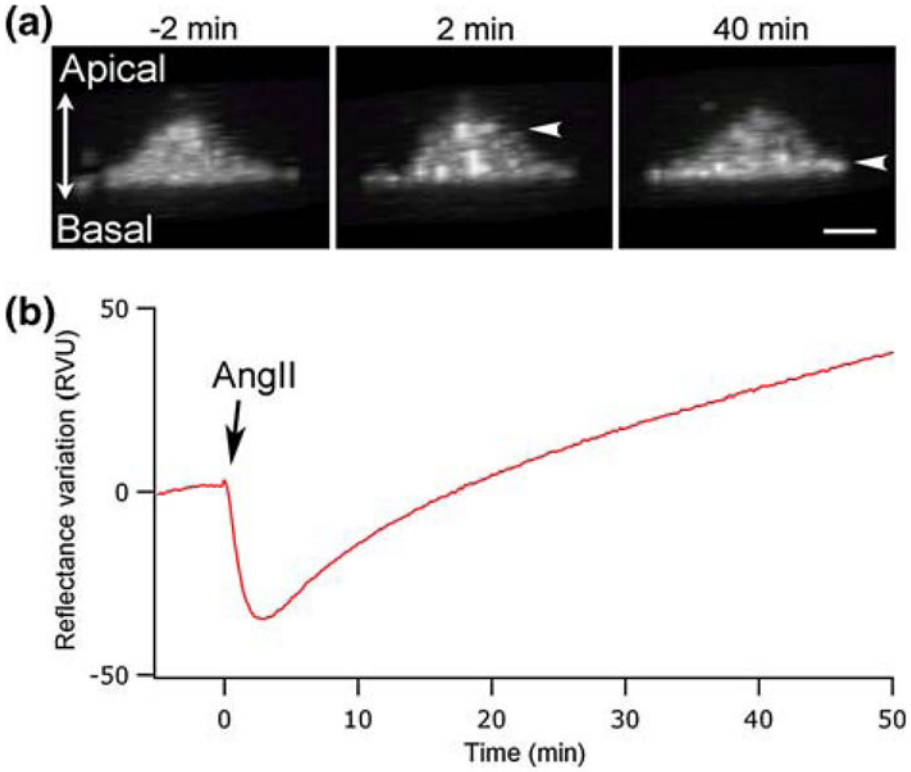

FIGURE 4.

Confocal imaging of HEK-293 cells, transfected with GFP-actin, in relation to the SPR signal. (a) Confocal transversal view of an individual cell, constructed from 55 sections of 250 nm. Micrographs are presented at selected times before and after AngII stimulation (−2, 2 and 40 min). (b) SPR signal associated with the stimulation of cells by 100 nM AngII. The scale bar corresponds to 10 μm.

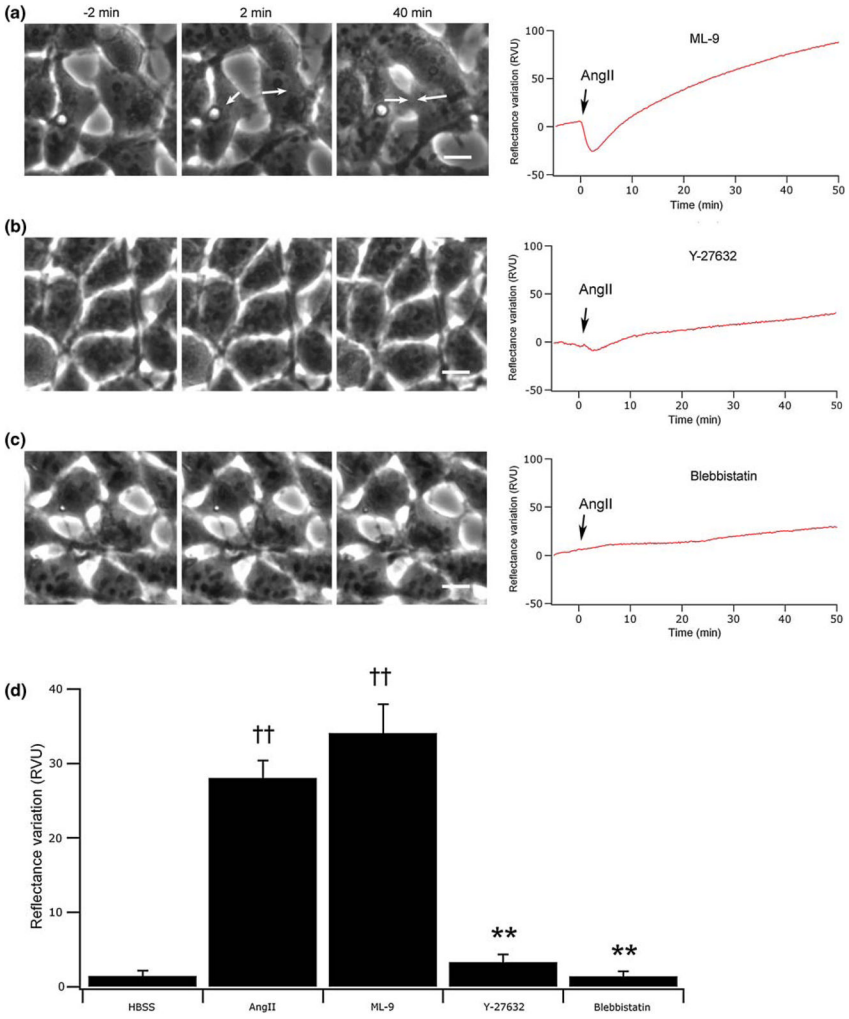

FIGURE 5.

Implication of signaling pathways influencing the actin cytoskeleton in the SPR signal variation. In (a), (b) and (c) are presented phase-contrast micrographs recorded before (−2 min) and after AngII stimulation (2 and 40 min) for cell treatment with inhibitors targeting respectively the MLCK (20 μM, ML-9), RhoK (10 μM, Y-27632) or directly the actomyosin contraction (100 μM, blebbistatin). (d) Summary of the amplitudes in the initial decrease of the SPR signal ($n = 5$). $^{\dagger\dagger}p<0.01$ versus HBSS stimulation, $^{**}p<0.01$ versus AngII stimulated cells. The scale bars correspond to 10 μm.

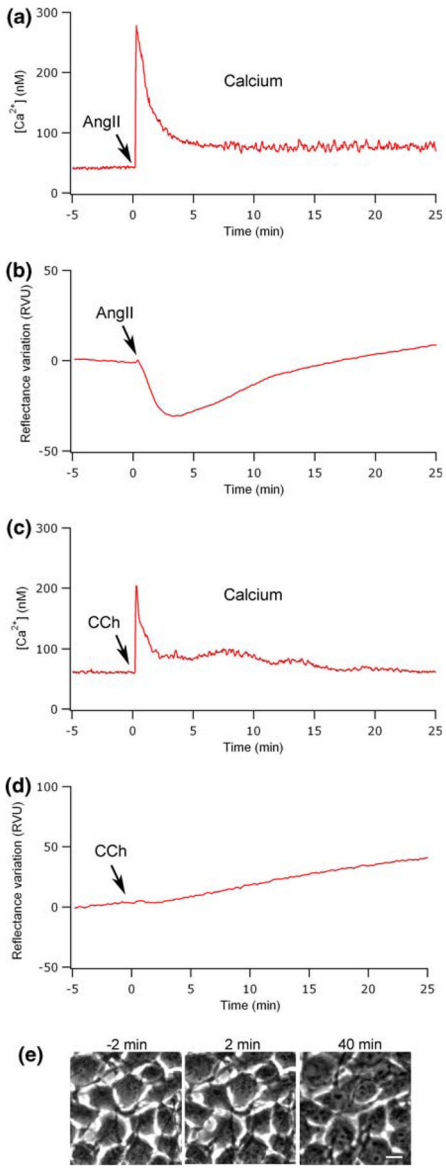

FIGURE 6.

Influence of the intracellular calcium mobilization on the SPR reflectance variations. The monitoring of intracellular calcium mobilization shows a characteristic transitory increase that reaches a maximum a few seconds after the addition of 100 nM AngII (a) or 10 μM CCh (b). SPR signal associated with the stimulation of cells by AngII (b) or CCh (d). Phase-contrast micrographs (e) recorded before (−2 min) and after CCh stimulation (2 and 40 min). The scale bar corresponds to 10 μm.